Available online at www.sciencedirect.com
ScienceDirect
Applied Surface Science 253 (2007) 8245–8249
applied surface science
www.elsevier.com/locate/apsusc

Diamond-like carbon coated ultracold neutron guides

S. Heule [a,b,*], F. Atchison [a], M. Daum [a], A. Foelske [a], R. Henneck [a], M. Kasprzak [a,c], K. Kirch [a], A. Knecht [a,b], M. Kuźniak [a,d], T. Lippert [a], M. Meier [a], A. Pichlmaier [a], U. Straumann [b]

[a] Paul Scherrer Institut (PSI), 5232 Villigen PSI, Switzerland
[b] Physik-Institut der Universität Zürich, Switzerland
[c] Stefan Meyer Institut für subatomare Physik, Austrian Academy of Sciences, Vienna, Austria
[d] Jagellonian University, Cracow, Poland

Available online 27 February 2007

Abstract

It has been shown recently that diamond-like carbon (DLC) with a sp^3 fraction above 60% is a better wall coating material for ultracold neutron applications than beryllium. We report on results of Raman spectroscopic and XPS measurements obtained for diamond-like carbon coated neutron guides produced in a new facility, which is based on pulsed laser deposition at 193 nm. For diamond-like carbon coatings on small stainless steel substrates we find sp^3 fractions in the range from 60 to 70% and showing slightly increasing values with laser pulse energy and pulse repetition rate.

PACS : 79.20.Ds; 14.20.Dh; 78.30.Jw; 33.60.Fy

Keywords: Diamond-like carbon; Characterization methods; sp^3 bonding; Pulsed laser deposition; Ultracold neutrons

1. Introduction

Ultracold neutrons (UCN) are free neutrons with velocities up to 8 m/s and corresponding energies of up to ~300 neV. They can be described as an ideal gas with a temperature of several milli-Kelvin [1]. Their trajectories are affected by gravitation, by magnetic fields and by the strong interaction with nuclei. The strong interaction can be described by defining a pseudo potential for each material, called the Fermi potential [1,2]:

$$V = \frac{2\pi\hbar^2}{m_n} Nb \tag{1}$$

Here, m_n is the neutron mass, N the scattering center density and b the bound coherent nuclear scattering length. Neutrons with kinetic energy below the Fermi potential of a material, V, or below the critical velocity, $v_C = \sqrt{2V/m_n}$, are reflected under any angle of incidence. Materials with high Fermi potential are e.g. diamond (306 neV), beryllium (251 neV) and nickel (245 neV), where the values have been calculated with Eq. (1) using Ref. [3] for '*b*'.

Another important item is the loss coefficient, η, which contributes linearly to the loss probability per wall collision. As the UCN are in the low energy tail of a Maxwellian distribution the spectral probability is proportional to kinetic energy and therefore, the ideal material for UCN applications has a high Fermi potential and a low loss coefficient. A recent experiment obtained at room temperature shows a loss probability of $\eta = (3.5 \pm 0.1) \times 10^{-4}$ for DLC and $\eta = (4.2 \pm 0.3) \times 10^{-4}$ for beryllium [4]. These values are among the best measured for high Fermi potential materials without any special surface pre-treatment. Beryllium has been widely used in the past, although it is toxic. In order to reduce the amount of material needed, coatings are usually used instead of solids. Large areas have to be coated for typical UCN applications and the coatings have to cover the substrate surface homogeneously and without holes. The thickness of the coatings should be in the range of 100–300 nm, being one order of magnitude thicker than the typical penetration depth of UCN upon wall reflection. Also, contamination of the coatings by neutronically bad materials, e.g. hydrogen, needs to be avoided. Within the last few years, diamond-like carbon (DLC) has been successfully tested as wall coating material in UCN applications (see e.g. Refs. [4–6]). The

* Corresponding author at: Paul Scherrer Institut (PSI), 5232 Villigen PSI, Switzerland. Tel.: +41 56 310 32 67; fax: +41 56 310 32 94.
E-mail address: stefan.heule@psi.ch (S. Heule).

0169-4332/$ – see front matter
doi:10.1016/j.apsusc.2007.02.139

coatings described in Ref. [5] were produced by chemical vapor deposition (CVD) using natural methane and deuterated methane as precursor gas. They had a comparatively low density of 2.1 g/cm^3, measured by neutron reflectometry and the value for V was 220 neV. No measurement of η for these coatings was reported.

The coatings in Refs. [4] were produced by laser-induced vacuum arc deposition [7]. As a physical vapor deposition (PVD) method, deposition is achieved by evaporating a pure graphite target. As the amount of hydrogen in such high-purity graphite is negligible, hydrogen-free DLC coatings can be produced. The coatings had a sp^3 fraction of up to 65%, determined by XPS (see also [8]). Applying the relation obtained in Ref. [9],

$$\rho\,(\mathrm{g/cm^3}) = 1.92 + 1.37k, \tag{2}$$

where k is the sp^3 fraction, gives a film density of 2.81 g/cm^3. The corresponding Fermi potential, obtained by UCN transmission [8], was 249 neV, equal to that of Be coated silicon which was measured in the same experiment. Diamond-like carbon coatings with higher sp^3 fractions [10] have been produced using pulsed laser deposition (PLD). An excimer laser with 248 nm wavelength and a short focal length (33 cm) optical system was used to ablate a graphite target. Critical velocities of up to 7 m/s ($V \approx 256$ neV) were obtained. A longer focal length (1.5 m) was used for the deposition of DLC on the inside of tubes and resulted in significantly lower values ($v_C \approx 6.5$ m/s, $V \approx 220$ neV).

At PSI, we are building a coating facility for UCN guides based on PLD, using an excimer laser at 193 nm wavelength, as smaller laser fluences are sufficient at shorter wavelengths for the production of DLC films with a high sp^3 fraction (see e.g. [11]). Pulsed laser deposition at short wavelength can produce thin films of uniform thickness [11]. Together with a smooth substrate this leads to small surface roughness of the UCN guide, which is essential for obtaining a high transport efficiency in guides. A rough surface enhances the contribution of diffuse reflection, which leads to increased angles of incidence for UCN-wall collisions. Thus, the velocity component normal to the surface increases and more UCN are not reflected, i.e. are lost.

The DLC-coated guides produced with the setup described below will be used for the new high-intensity source for UCN presently under construction at PSI [12].

2. Experimental

2.1. Tube coating setup

The setup consists of three main parts: laser, optics and the deposition chamber. The distances between the three parts are kept as small as possible. Fig. 1 shows a schematic layout of the setup.

The pulsed laser beam with 193 nm wavelength (item 1 in Fig. 1) is produced by an excimer laser (Lambdaphysik LPX-301, item 2). The pulse length is about 23 ns, the beam profile is roughly rectangular with dimensions of about 23 mm × 4 mm.

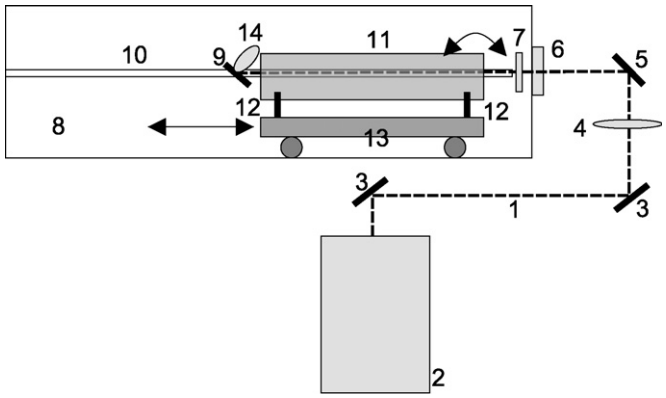

Fig. 1. Schematic overview of the tube PLD coating facility (not to scale). (1) laser beam, (2) excimer laser, (3) fixed mirrors, (4) focussing UVFS lens, (5) fast steering mirror, (6) UVFS viewport, (7) UVFS viewport protection disc, (8) vacuum chamber, (9) graphite target, (10) target tube, (11) substrate tube, (12) wheels for substrate tube rotation, (13) substrate trolley and (14) ablation plume.

The maximum pulse energy obtained at a repetition rate of 10 Hz is about 550 mJ. Excimer lasers have a large divergence which leads to large spot size if the laser beam is focussed by a lens with long focal length (of the order 1.5 m). The result is a moderate laser power density, too low to produce DLC films with high sp^3 fraction. Therefore, our laser is equipped with unstable resonator optics which should deliver a nominal divergence of 0.4 mrad for each dimension of the beam [13], although the laser intensity drops to 50%. The resulting gain factor for focal lengths around 1.5 m can be up to 20.

The laser is deflected by two fixed mirrors (item 3) and focussed by an ultra violet grade fused silica (UVFS) lens with a focal length of 1260 mm (item 4). It is then deflected again by a fast steering mirror system (item 5) and enters the cylindrical coating chamber with 400 mm diameter (item 8) through a UVFS vacuum viewport (item 6) mounted at one end. Inside the chamber the beam passes another UVFS disc (item 7) which prevents the viewport from being coated by the ablated graphite. The focussed beam finally hits the target (item 9), a plate of spectroscopically pure graphite with a density of 2.21 g/cm^3, mounted inside a half opened tube (item 10) in such a way that the laser beam hits the target surface at an angle of 35°. The position where the laser beam hits the target is changed after each pulse by moving the fast steering mirror to achieve a homogeneous ablation of the graphite. Inside the vacuum chamber, the substrate tube (item 11) is mounted on a trolley (item 13). The trolley moves on rails (not shown), which allow translation of the substrate tube along the ablation plume (item 14); wheels (item 12) on top of the trolley allow the substrate tube to be rotated simultaneously. Both movements are driven by in-vacuum stepper motors.

The vacuum chamber has a total length of 2.5 m and is divided into three sections. This allows the coating of 1 m long tubes with diameters between 60 and 250 mm. For the production of the small test samples (see below), only the central part of the vacuum chamber with 91 cm length was used. A correspondingly short target tube was mounted, electrically insulated by polytetrafluoroethylene (PTFE) from

the chamber, which was set to ground. The chamber is evacuated by a combined system of a roots pump and a cryo pump. A pressure of 2×10^{-6} Pa could be achieved without any special cleaning or heating of the vacuum vessel.

A special substrate holder was built for the production of flat test samples with 10 mm × 10 mm and 20 mm × 20 mm size. It is equipped with a rotary motion feedthrough to allow three DLC films to be deposited without breaking vacuum. The holder is mounted from the top of the vacuum chamber in such a way that the substrate surface encloses an angle of 35° with the surface of the graphite target. For the tests reported here, the average distance between the graphite target and the substrate was fixed at about 6 cm (small variations are caused by the systematic change of the target spot location), as previous investigations with another PLD setup showed no dependence of the sp^3 fraction on the target-to-substrate distance [14]. Major parts of the substrate holder are made out of PTFE in order to electrically insulate the substrates from the vacuum vessel.

The substrates not being coated are protected by an aluminium mask with a hole (diameter 3 cm). An aluminium electrode is embedded in a piece of PTFE at one end of the mask and connected from the back, making it the anode for an in situ glow discharge cleaning system.

Most functions of the tube PLD coating setup, such as monitoring pressure and temperature, synchronisation of the fast steering mirror with laser pulses and pressure regulation are controlled by a central LabVIEW application [15].

2.2. Test sample production

As mentioned above, flat test samples of 1 cm^2 size were produced by coating stainless steel substrates with an averaged roughness of 40 nm. This roughness represents the best achievable value for the inner wall of stainless tubes commercially available, realized by electro-polishing. In order to work under conditions as close to the final application (tubes), the roughness of the flat test samples was determined to be the same, although lower roughness was available.

The influence of the process parameters pressure, pulse repetition rate and energy was studied by producing sample series with variation of one process parameter. The total laser energy was varied by using different high voltages for running the excimer laser. Each film was grown using 3000 pulses. The number of pulses was derived from previous results of test samples produced in another PLD coating chamber [14].

2.3. Sample characterization

The sp^3 fraction of the test samples was measured with two different methods: Raman spectroscopy and X-ray photoelectron spectroscopy (XPS). These two methods were found to be most suitable for DLC coatings used in UCN applications [16].

The Raman measurements were performed on a Dilor LabRam spectrometer. The excitation light source was a HeNe laser at 632.8 nm with a power of 25 mW. A grating with 1800 lines/mm and a magnification of 50 was used. The XPS measurements were performed on an ESCALAB 220i XL spectrometer using an Al Kα monochromatic X-ray source.

Thickness measurements were performed with a profilometer (Ambios XP-1) using a sharp edge of the coating. The roughness of both coated samples and uncoated substrates was also determined with the same instrument. An additional thickness control was performed with the Raman spectrometric measurements, as they would reveal insuffienctly thick (for UCN applications) DLC coatings [16].

3. Results

Following the recently developed characterization procedure for DLC to be used as UCN wall coating material [16], each sample was first measured by Raman spectroscopy. The spectra were fitted with a Breit–Wigner–Fano (BWF) curve, corresponding to the Raman G band, a Lorentz curve describing the Raman D band and a linear background [17]. For the intensity ratio $I(D)/I(G)$, we found values below 5% for all samples. According to Ref. [18], the coatings can therefore be considered as hydrogen-free amorphous carbons (a-C) with a sp^3 fraction $\geq$20%. For most of the investigated samples Raman spectra could be obtained. These films are therefore thick enough for use as wall coatings in UCN applications. The samples with insufficient film thickness were not used for further characterization.

The XPS analysis was performed with the XPSPeak software [19] and followed Ref. [20]. The values for the sp^3 fraction range from 40 to 70%. The values and (statistical) errors in Fig. 2 constitute an average over two independent measurements performed at two different locations on the samples (one central and one peripheral).

One process parameter studied was the laser energy on the graphite target per pulse. It was varied from 50 to 200 mJ. The laser repetition rate was set to 10 Hz, the pressure was kept at 1×10^{-4} Pa (stabilized by adding argon). The XPS results for the sp^3 fraction, which are shown in Fig. 2a, show slightly higher values for higher energies. It is difficult to determine the energy density on the target as the specific combination of the laser cavity with the unstable resonator optics causes diffraction effects which result in a focus spot with badly determined intensity distribution.

Another process parameter studied was the laser repetition rate, which was varied from 5 to 50 Hz. The laser energy per pulse was kept around 80 mJ, the pressure inside the chamber at 1×10^{-4} Pa. The XPS measurements show a small but systematic increase of the sp^3 fraction with increasing repetition rate, as shown in Fig. 2b.

The profilometric measurements showed average roughnesses, R_a, of the order of 40 nm for the uncoated substrates and also for the coated samples, which agrees with Ref. [11]. The thickness of the coatings could be determined only for a part of the test samples, as most of the substrates were quite uneven. In addition, the edges of the coatings were relatively smooth, leading to correspondingly smooth steps in the height profiles. Nevertheless, the results obtained showed coating thicknesses

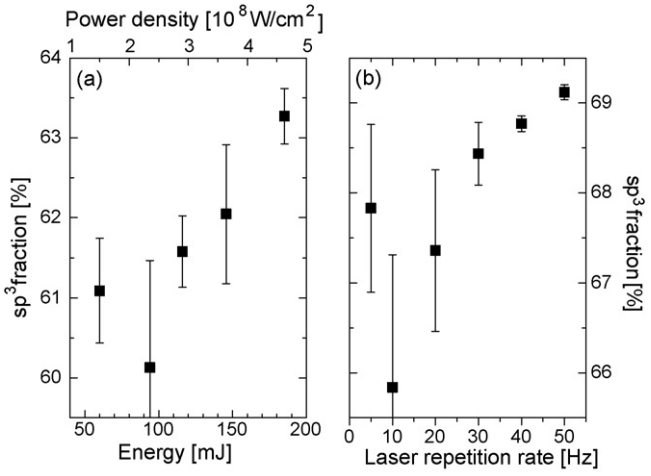

Fig. 2. Results of XPS measurements for test sample series with (a) varied energy, deposited at 10 Hz and (b) varied laser repetition rate, deposited with a laser energy of ∼80 mJ. A background atmosphere of 10^{-4} Pa argon was used for both series. The error bars result from the statistical uncertainties of the XPS measurements; the large variation in the uncertainty is due to the fact that for each data point two measurements at different locations on the sample were averaged. For (a) the resulting power density of the laser beam on the target is plotted on the top axis, although the values have to be considered as estimation due to the inhomogeneous laser spot (see text).

in the range of 50–150 nm, which is sufficient for UCN applications.

4. Discussion

The results described in Section 3 show that slightly increased sp^3 fractions are obtained with higher laser energies. This agrees with findings in e.g. Ref. [21]. The inhomogeneous laser spot on the target makes an estimation of the energy and power density difficult. We estimate the area of the central spot without the diffraction pattern to be about 1.7 mm^2. Assuming 80% of the total energy to be concentrated in this central spot, we calculate an energy density of ∼5 J/cm^2 and a power density of $\sim 2 \times 10^8$ W/cm^2 for the central spot using a total laser energy per pulse of 100 mJ. It is not known if the energy in the central spot is linearly dependent on the total laser energy, i.e. if a factor 2 higher total laser energy also results in doubling the energy density of the central spot. The sp^3 fraction may also be limited by the tails of the laser beam with lower energy density producing ablated particles with lower kinetic energies. Caused by these tails, the target area illuminated with low energy density, just high enough to be above the ablation threshold energy density of graphite, is expected to increase with increasing total laser energy. This results in a different ratio of high-energy density and low-energy density area for different laser energies. However, isolating the central spot by a fixed mask, i.e. blocking the outer part of the beam, is not possible due to the change of the laser spot position on the target with each pulse.

The highest sp^3 fractions were measured for coatings deposited at high repetition rates. An increase of the diamond crystallite size with increasing repetition rate [22] as well as an increase of the sp^2 ordering with decreasing repetition rate [23] has been observed previously. Whether these and our observation have the same origin cannot be evaluated with the limited data set available, but one possible explanation could be an increase of the target temperature. A higher temperature of the graphite target due to higher repetition rates could cause an increase in kinetic energy of the ablated species and therefore be the origin of the larger sp^3 content. It is planned to test this hypothesis by varying the target temperature.

The highest sp^3 fraction measured was close to 70%. The corresponding film density, calculated by Eq. (2), is 2.88 g/cm^3, the corresponding Fermi potential 250 neV. This is equivalent to the theoretical value of beryllium. There is still room for improvements, as, according to Eq. (2), the highest density for hydrogen-free amorphous carbon films, with a sp^3 fraction of 100%, is ∼3.3 g/cm^3 which would have a Fermi potential of ∼285 neV. We will therefore continue the optimization of the production process parameters by e.g. investigating the influence of a bias voltage applied between target and substrate.

5. Conclusions

We have produced test samples with sp^3 fractions up to about 70% by pulsed laser deposition with an excimer laser at 193 nm wavelength. The corresponding Fermi potential is close to 250 neV. The test samples were produced in a PLD coating facility which is built up for coating the inside of tubes in order to use them as guides for ultracold neutrons. We find that increasing the laser energy and the repetition rate produces films with higher sp^3 fractions.

Acknowledgements

This work was performed at the Paul Scherrer Institut, Villigen, Switzerland. We are grateful to M. Müller, U. Bugmann and collaborators for their excellent work in fabrication of the experimental equipment. We appreciate the valuable discussions with L. Hardwick, R. Koetz, G. Kopitkovas, C.-F. Meyer, B. Schultrich and L. Urech. We thank M. Nagel for giving us the possibility to perform the profilometric measurements. This work is supported by the Swiss National Science Foundation (grant 200021-105400).

References

[1] V.K. Ignatovich, The Physics of Ultracold Neutrons, Oxford University Press, Oxford, 1990.
[2] R. Golub, D.J. Richardson, S.K. Lamoreaux, Ultra-Cold Neutrons, Adam Hilger, Bristol, 1991.
[3] NIST Center for neutron research, http://www.ncnr.nist.gov/resources/n-lengths/
[4] F. Atchison, T. Bryś, M. Daum, P. Geltenbort, R. Henneck, S. Heule, M. Kasprzak, K. Kirch, A. Pichlmaier, C. Plonka, U. Straumann, C. Wermelinger, Phys. Lett. B 625 (2005) 19.
[5] M. van der Grinten, J. Pendlebury, D. Shiers, C. Baker, K. Green, P. Harris, P. Iaydjiev, S. Ivanov, P. Geltenbort, Nucl. Instrum. Methods A 423 (1999) 421.

[6] T. Brys, M. Daum, P. Fierlinger, P. Geltenbort, D. George, M. Gupta, R. Henneck, S. Heule, M. Horvat, M. Kasprzak, K. Kirch, K. Kohlik, M. Negrazus, A. Pichlmaier, U. Straumann, V. Vrankovic, C. Wermelinger, Nucl. Instrum. Methods A 550 (2005) 637.
[7] H.-J. Scheibe, B. Schultrich, Thin Solid Films 246 (1994) 92.
[8] F. Atchison, B. Blau, T. Bryś, M. Daum, P. Fierlinger, A. Foelske, P. Geltenbort, M. Gupta, R. Henneck, S. Heule, M. Kasprzak, M. Kuźniak, K. Kirch, M. Meier, A. Pichlmaier, C. Plonka, R. Reiser, B. Theiler, O. Zimmer, G. Zsigmond, Phys. Lett. B 642 (2006) 24.
[9] A.C. Ferrari, A. Libassi, B.K. Tanner, V. Stolojan, J. Yuan, L.M. Brown, S.E. Rodil, B. Kleinsorge, J. Robertson, Phys. Rev. B 62 (2000) 11089.
[10] M. Makela, Ph.D. thesis, Virginia Polytechnic Institute and State University, 2005.
[11] A.A. Voevodin, M.S. Donley, Surf. Coat. Technol. 82 (1996) 199.
[12] http://ucn.web.psi.ch
[13] http://www.coherent.com/Lasers/
[14] T. Bryś, M. Daum, P. Fierlinger, A. Foelske, M. Gupta, R. Henneck, S. Heule, M. Kasprzak, K. Kirch, M. Kuźniak, T. Lippert, M. Meier, A. Pichlmaier, U. Straumann, Diamond Relat. Mater. 15 (2006) 928.
[15] http://www.labview.com, http://www.ni.com
[16] F. Atchison, T. Bryś, M. Daum, P. Fierlinger, A. Foelske, M. Gupta, R. Henneck, S. Heule, M. Kasprzak, K. Kirch, R. Kötz, M. Kuźniak, T. Lippert, C.-F. Meyer, F. Nolting, A. Pichlmaier, D. Schneider, B. Schultrich, P. Siemroth, U. Straumann, Diamond Relat. Mater. 16 (2007) 334.
[17] S. Prawer, K.W. Nugent, Y. Lifshitz, G.D. Lempert, E. Grossman, J. Kulik, I. Avigal, R. Kalish, Diamond Relat. Mater. 5 (1996) 433.
[18] A.C. Ferrari, J. Robertson, Phys. Rev. B 64 (2001) 075414.
[19] R. Kwok, XPS Peak, download at http://www.phy.cuhk.edu.hk/~surface/XPSPEAK/
[20] P. Merel, M. Tabbal, M. Chaker, S. Moisa, J. Margot, Appl. Surf. Sci. 136 (1998) 105.
[21] T. Witke, T. Schuelke, J. Berthold, C.F. Meyer, B. Schultrich, Surf. Coat. Technol. 116 (1999) 609.
[22] T. Yoshitake, T. Hara, K. Nagayama, Diamond Relat. Mater. 12 (2003) 306.
[23] H. Nakazawa, Y. Yamagata, M. Suemitsu, M. Mashita, Thin Solid Films 467 (2004) 98.